

# Increased paclitaxel cytotoxicity against cancer cell lines using a novel functionalized carbon nanotube

Z Sobhani<sup>1</sup>  
R Dinarvand<sup>1,2</sup>  
F Atyabi<sup>1,2</sup>  
M Ghahremani<sup>3</sup>  
M Adeli<sup>4,5</sup>

<sup>1</sup>Department of Pharmaceutics,  
<sup>2</sup>Nanotechnology Research Center,  
<sup>3</sup>Department of Pharmacology and Toxicology, Faculty of Pharmacy, Tehran University of Medical Sciences, Tehran; <sup>4</sup>Department of Chemistry, Sharif University of Technology, Tehran; <sup>5</sup>Department of Chemistry, Faculty of Science, Lorestan University, Khoramabad, Iran

**Abstract:** Potential applications of carbon nanotubes have attracted many researchers in the field of drug delivery systems. In this study, multiwalled carbon nanotubes (MWNTs) were first functionalized using hyperbranched poly citric acid (PCA) to improve their hydrophilicity and functionality. Then, paclitaxel (PTX), a potent anticancer agent, was conjugated to the carboxyl functional groups of poly citric acid via a cleavable ester bond to obtain a MWNT-g-PCA-PTX conjugate. Drug content of the conjugate was about 38% (w/w). The particle size of MWNT-g-PCA and MWNT-g-PCA-PTX was approximately 125 and 200 nm, respectively. Atomic force microscopy and transmission electron microscopy images showed a curved shape for MWNT-g-PCA and MWNT-g-PCA-PTX, which was in contrast with the straight or linear conformation expected from carbon nanotubes. It seems that the high hydrophilicity of poly citric acid and high hydrophobicity of MWNTs led to conformational changes from a linear state to a curved state. Paclitaxel can be released from the MWNT-g-PCA-PTX conjugates faster at pH 6.8 and 5.0 than at pH 7.4, which was suitable for the release of the drug in tumor tissues and tumor cells. In vitro cytotoxicity studies were evaluated in the A549 and SKOV3 cell lines. MWNT-g-PCA had an insignificant cytotoxic effect on both cell lines. MWNT-g-PCA-PTX had more of a cytotoxic effect than the free drug over a shorter incubation time (eg, 24 hours versus 48 hours), which suggests improved cell penetration of MWNT-g-PCA-PTX. Therefore, paclitaxel conjugated to MWNT-g-PCA is promising for cancer therapeutics.

**Keywords:** multiwalled carbon nanotubes, functionalization, anticancer, drug delivery, nanoparticles

## Introduction

Carbon nanotubes, discovered in 1991 by the Japanese electron microscopist Sumio Iijima, opened up new opportunities in the field of nanotechnology and nanoscience.<sup>1-3</sup> The interesting properties of carbon nanotubes, such as stability, inertness, and higher surface area-to-volume ratio than spheres (providing high loading capacity for guest molecules), suggest the potential utility of these materials as carriers in drug delivery systems requiring higher loadings of therapeutic agents.<sup>4-6</sup> The application of carbon nanotubes in drug delivery systems was apparent immediately after the first demonstration of the capacity of these materials to penetrate into cells.<sup>7</sup> Several in vitro studies have demonstrated that carbon nanotubes can effectively transport various molecules including drugs, peptides, and proteins into cells.<sup>8-13</sup>

High hydrophobicity, low functionality, and the large size of pure carbon nanotubes limit their biological applications. Therefore, modification of carbon nanotubes through covalent or noncovalent functionalization of their external walls

Correspondence: F Atyabi  
Faculty of Pharmacy Teheran University  
of Medical Sciences, Teheran, Iran  
Tel +98 21 6695 9052  
Email atyabifa@tums.ac.ir

is a key step for biomedical applications because a wide variety of active molecules can be linked to a functionalized carbon nanotube.<sup>14–18</sup> The ultra high surface area of these macromolecules is appropriate for efficient loading of chemotherapy drugs.<sup>11,19</sup> Although the various functionalizations of carbon nanotubes have been successfully achieved, only a few examples of delivery of small molecules (antiviral, antibacterial, and anticancer agents) using functionalized carbon nanotubes have been reported.<sup>16,20,21</sup>

Polyethylene glycol has been popular as a means of functionalization of carbon nanotubes in drug delivery systems.<sup>22,23</sup> Due to the hydrophilicity of polyethylene glycol, this polymer is used to prepare stealth nanoparticles to escape reticuloendothelial systems. The long circulation time facilitates passive targeting to the cancer cells through the enhanced permeability and retention effect of tumor blood vessels.<sup>24</sup> Liu et al loaded doxorubicin onto pegylated single-walled carbon nanotubes<sup>11</sup> and also covalently conjugated paclitaxel to branched polyethylene glycol segments which were adsorbed on the side walls of carbon nanotubes.<sup>25</sup> However, polyethylene glycol with limited arms was commonly used for functionalization of carbon nanotubes to conjugate to other molecules for drug delivery systems. In this study, hyperbranched poly citric acid (PCA) with a high capacity for conjugation to drug molecules was used for the functionalization of multiwalled carbon nanotubes (MWNTs).

The shape and size of nanoparticles are two critical factors that affect the toxicity and efficiency of drug delivery systems. However, the shape, size, and conformation of the drug delivery systems based on carbon nanotubes have not been investigated in depth.

In this report, we propose a novel drug delivery system for cancer chemotherapy based on multiwalled carbon nanotubes functionalized with hyperbranched poly citric acid (MWNT-g-PCA) and conjugated to the commonly used potent chemotherapy drug, paclitaxel (PTX), to produce a MWNT-g-PCA-PTX conjugate. As described previously, these carbon nanotubes can be taken up by cells through endocytosis, where the cleavable ester bond between paclitaxel and poly citric acid is hydrolyzed and paclitaxel is released into the cytoplasm. Thus, we determined the morphology, size, and cytotoxicity of MWNT-g-PCA-PTX conjugates. We found that the conformation of MWNT-g-PCA changes from a straight to curved nanostructure. In addition, cytotoxicity studies revealed that the MWNT-g-PCA-PTX conjugate increased the cytotoxicity of the drug.

## Methods

### Functionalization of MWNTs with poly citric acid

Multiwalled carbon nanotubes (number of walls 3–15, outer diameter 5–20 nm, length 1–10  $\mu\text{m}$ ) were purchased from Plasmachem GmbH, Berlin, Germany. MWNT-g-PCA was synthesized according to procedures reported in the literature.<sup>26,27</sup> Briefly, 1 g of MWNTs was mixed with 20 mL of concentrated  $\text{HNO}_3$  and  $\text{H}_2\text{SO}_4$  (1:3 ratio), and the mixture was sonicated for 30 minutes and refluxed for 24 hours at 100°C. The resulting black mixture was then diluted with 1 L of distilled water, filtered, and washed with deionized water to adjust the pH to 6. The filtrate was dried in a vacuum oven for 24 hours at 40°C. Then, 0.1 g of oxidized MWNTs and 2.5 g of monohydrated citric acid was added to a polymerization ampoule equipped with a magnetic stirrer and a vacuum inlet. The mixture was heated to 100°C while stirring for 30 minutes. After removing water via the vacuum inlet, the reaction temperature was gradually increased to 140°C over four hours, while the dynamic vacuum was operated at proper intervals. The product was cooled and then dissolved in tetrahydrofuran. Free citric acid was precipitated in cyclohexane.

### Synthesis of MWNT-g-PCA-PTX conjugate

MWNT-g-PCA (50 mg), N-(3-dimethylamino propyl)-N-ethylcarbodiimide hydrochloride (EDC) (23 mg, 0.12 mmol) and 4-(dimethylamino) pyridine (DMAP) (15 mg, 0.12 mmol) were dissolved in 5 mL of anhydrous dimethylformamide. The mixture was then stirred at 0°C for 30 minutes. Anhydrous dimethylformamide (5 mL) containing paclitaxel (50 mg, 0.06 mmol) was then added to the mixture and stirred for 24 hours at 0°C. Precipitate was filtered out and the filtrate was dialyzed (molecular weight cutoff 1200 Da, Sigma-Aldrich Corp St. Louis, MO) against dimethylformamide overnight to remove untreated materials. The dialyzed solution was then dried under nitrogen stream for four hours. The reaction process between paclitaxel and activated MWNT-g-PCA was carried out at different times (24, 48, and 72 hours) and at different drug to carrier ratios (0.1/1, 0.5/1, 1/1, and 2/1 w/w) to obtain the optimum drug content and reaction yield.

### Characterization techniques

The CNT-g-PCA-PTX conjugate was characterized using infrared,  $^1\text{H}$  nuclear magnetic resonance (NMR),  $^{13}\text{C}$  NMR,

differential scanning calorimetry, dynamic light scattering, and microscopic techniques as follows: infrared (Perkin-Elmer Spectrum GX, Waltham, MA) was used to analyze the changes in the surface chemical bonding and structure, using KBr discs of each sample in the frequency range of 4000–400  $\text{cm}^{-1}$ .  $^1\text{H}$  NMR spectra were recorded in dimethyl sulfoxide solution on Bruker DRX 500 (500 MHz [Bruker Corporation, Billerica, MA]) apparatus with the solvent proton signal for reference.  $^{13}\text{C}$  NMR spectra were recorded on the same instrument using the solvent carbon signal as a reference. Differential scanning calorimetry was used to determine the thermal behavior of the conjugated nanotubes. Differential scanning calorimetry analysis was performed with a Mettler DSC 823-e (Mettler Toledo GmbH, Greifensee, Switzerland) instrument using Mettler Stare software version 9.x. Indium was used to calibrate the instrument. Samples weighing approximately 10 mg were heated in a hermetically sealed aluminum pan at a rate of  $10^\circ\text{C}/\text{min}$  in a temperature range of  $25\text{--}400^\circ\text{C}$  under a nitrogen atmosphere.

Particle size and polydispersity of the MWNT-*g*-PCA and MWNT-*g*-PCA-PTX conjugates were determined by dynamic light scattering (Zetasizer Nano-ZS Malvern Instruments, Malvern, UK), fitted with particle size analysis software (Dispersion Technology software v 4.2) at  $25^\circ\text{C}$ .

The shape and surface morphology of the conjugate nanostructures were evaluated by atomic force microscopy (Dualscope C-21, DME, Copenhagen, Denmark, with DME-SPM v2.1.1.2 software) and transmission electron microscopy (Philips CN10, [Philips, Eindhoven, the Netherlands] etherlands). Atomic force microscopy was performed in air under ambient conditions, and transmission electron microscopy analysis was performed at 100 kV.

## Paclitaxel content of the conjugate

The amount of paclitaxel loaded onto MWNT-*g*-PCA-PTX was quantified by an indirect method<sup>28</sup> whereby free paclitaxel after the reaction with MWNT-*g*-PCA that accumulated in the dialysis medium was analyzed. In this way, the amount of conjugated paclitaxel to the MWNT-*g*-PCA was estimated according to the initial amount of drug. This amount was presented as mass of drug in the conjugate according to the following equation. For high-pressure liquid chromatography analysis, samples (20  $\mu\text{L}$ ) were injected into a Knauer system (Model k 1001, WellChrom, [Dr. Ing. Herbert Knauer GmbH, Berlin, Germany]) equipped with an ultraviolet detector (UV Detector 2500). Isocratic chromatography was performed on a C-18 column (4.6 mm  $\times$  25 cm) with 5  $\mu\text{m}$  packing (Knauer) using acetonitrile/water (60:40 v/v) as a mobile

phase. Paclitaxel was detected at 227 nm. Drug content was calculated by the following equation:

$$\text{Drug content (\%W/W)} = \frac{\text{Mass of drug in conjugate}}{\text{Mass of conjugate}} \times 100$$

## In vitro drug release

The pattern of drug release from the MWNT-*g*-PCA nanostructures was studied in deionized water and phosphate buffers at pH 5.0, 6.8, and 7.4 containing 0.1% (w/v) Tween 80 as medium.<sup>29</sup> The correct amount of MWNT-*g*-PCA-PTX (containing 1 mg of paclitaxel) dispersed in 10 mL of media containing 0.1% (w/v) Tween 80 was placed in a dialysis bag immersed in 100 mL of the release media, and was then placed in an incubator shaker set at 100 rpm and  $37^\circ\text{C}$ . At predetermined time intervals, 10 mL of the release medium was removed and replaced with fresh medium. Samples were diluted with acetonitrile (1:1 ratio) and the paclitaxel released was determined by high-pressure liquid chromatography as described.

## In vitro cytotoxicity

The cytotoxicity of MWNT-*g*-PCA-PTX, MWNT-*g*-PCA, and free paclitaxel was assessed by standard MTT assay. SKOV3 ovary cancer cells and A549 lung cancer cells were cultured in RPMI-1640 medium supplemented with 10% fetal bovine serum and 1% penicillin-streptomycin at  $37^\circ\text{C}$  in a humidified incubator with 5%  $\text{CO}_2$ . Cells in the exponential growth phase were seeded in 96-well plates (Nunc, Denmark) at a density of  $1 \times 10^4$  viable cells/well. After overnight incubation, cells were exposed to different concentrations of free paclitaxel, MWNT-*g*-PCA-PTX, and MWNT-*g*-PCA in dimethyl sulfoxide at  $37^\circ\text{C}$  for predetermined times under standard cell culture conditions. At designated time intervals, 20  $\mu\text{L}$  of MTT (5 mg/mL) was added to each well and incubated for 3–4 hours. The formazan crystals in each well were then dissolved in 100  $\mu\text{L}$  of dimethyl sulfoxide. The absorbance of each well was measured with a microplate reader (Anthos 2020, [Anthos Labtec Instruments GmbH, Salzburg, Austria]) at 570 nm against 690 nm. The percentage of cell viability was calculated according to the following equation:

$$\text{Cell viability \%} = \frac{\text{Abs 570nm of treated group}}{\text{Abs 570nm of control group}} \times 100$$

In all the cytotoxicity assays, cell treatments were assessed in triplicate and the results of three independent experiments were reported ( $n = 3$ ). The toxicity of the

MWNT-g-PCA-PTX and free paclitaxel was also expressed as the inhibitory concentration at which 50% of cell growth inhibition was obtained ( $IC_{50}$ ).

## Statistical analysis

Statistical analysis was performed using the Student's *t*-test for the two groups. All results were expressed as the mean  $\pm$  standard deviation (SD). A probability (*P*) of less than 0.05 was considered to be statistically significant.

## Results

### Synthesis of MWNT-g-PCA-PTX conjugate and structural characterization

Paclitaxel was conjugated to the carboxyl functional groups of the poly citric acid branches on the surface of MWNTs via a cleavable ester bond, forming a MWNT-g-PCA-PTX conjugate (Figure 1). The ester used in this study was prepared by the "active ester approach" method in *N,N*-dimethylformamide, using aminopropylcarbodiimide as the condensing agent and 4-dimethylaminopyridine as the base. The unconjugated paclitaxel was removed thoroughly from the MWNT-g-PCA-PTX solution by dialysis. The conjugation reaction of paclitaxel to MWNT-g-PCA was optimized for time, temperature, and drug/MWNT-g-PCA ratios. The reaction was completed in 24 hours and the optimal drug/MWNT-g-PCA ratio was 1/1 (w/w). In these conditions, the percentage of loaded drug or loading capacity was  $38\% \pm 7\%$  and the reaction yield was  $25\% \pm 2\%$  ( $n = 3$ ). When the drug/MWNT-g-PCA ratio was increased to 2:1, the drug content and reaction yield were slightly increased to  $40\% \pm 6\%$  and  $30\% \pm 4\%$ , respectively. The limited loading capacity for paclitaxel at a higher drug:carrier ratio may be related to high steric hindrance of paclitaxel (the infrared spectrum of samples were shown in supplementary data, Figure S1).

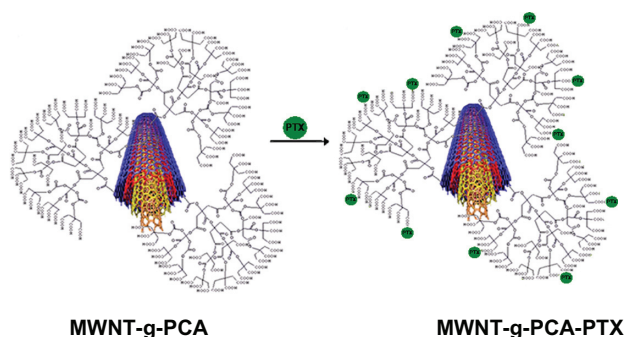


**Figure 1** Scheme of conjugated paclitaxel to MWNT-g-PCA.

**Abbreviations:** MWNT, multiwalled carbon nanotube; PCA, poly citric acid.

In the infrared spectrum of MWNT-g-PCA (see supplementary data, Figure S1-b), broad absorbance bands at  $3550\text{--}2400\text{ cm}^{-1}$  were assigned to the hydroxyl groups of poly citric acid branches grafted on the surface of MWNTs, while a relatively broad absorbance band at  $1750\text{--}1700\text{ cm}^{-1}$  corresponded to the carbonyl groups of oxidized MWNTs and acidic and esteric carbonyl groups of grafted poly citric acid. The infrared spectrum of paclitaxel (Figure S1-c) showed two characteristic bands at  $1736\text{ cm}^{-1}$  and  $1644\text{ cm}^{-1}$ , which were each assigned to its carbonyl groups and the  $C = O$  bonds of amide group, respectively. These two peaks appeared in the infrared spectrum of the MWNT-g-PCA-PTX conjugate (Figure S1-d). The absorbance bands at  $3400\text{--}3500\text{ cm}^{-1}$  corresponded to the hydroxyl groups of paclitaxel (Figure S1-c), and broad absorbance bands of hydroxyl groups of poly citric acid branches (Figure S1-b) were transformed into a single band at  $3380\text{ cm}^{-1}$  in the MWNT-g-PCA-PTX conjugate (Figure S1-d). These findings confirmed the reaction between paclitaxel and poly citric acid branches of MWNT-g-PCA through esteric bonds.

Conjugation of paclitaxel molecules to the surface of MWNTs by poly citric acid spacers could easily be proven through comparison of the  $^1\text{H}$  and  $^{13}\text{C}$  NMR spectra of paclitaxel, MWNT-g-poly citric acid, and MWNT-g-PCA-PTX (supplementary data Figure S2, S3). In the  $^1\text{H}$  NMR spectra of MWNT-g-PCA-PTX (Figure S2-c) conjugate, signals of poly citric acid branches appeared between 2.6–3.6 ppm, as could also be seen in the  $^1\text{H}$  NMR spectra of MWNT-g-PCA (Figure S2-b). In the  $^{13}\text{C}$  NMR of MWNT-g-PCA-PTX conjugate (Figure S3-c), the appearance of a new signal at 206 ppm (in comparison with MWNT-g-PCA and paclitaxel) showed attachment of the paclitaxel molecules to the carboxyl functional groups of poly citric acid branches through ester bonds.

The thermal behavior of the conjugated nanotubes was investigated using differential scanning calorimetry (Figure 2). The differential scanning calorimetry curve of paclitaxel (Figure 2B) showed an endothermic peak at  $220^\circ\text{C}$  and an exothermic peak at  $242^\circ\text{C}$  which were assigned to its melting and degradation points, respectively. The differential scanning calorimetry curve of MWNT-g-PCA (Figure 2A) showed two endothermic peaks about  $100\text{--}140^\circ\text{C}$  and  $180\text{--}250^\circ\text{C}$ . The first endothermic peak was attributed to the loss of water and decomposition of poly citric acid branches. The second peak indicated the collapse of MWNTs. The differential scanning calorimetry curve of MWNT-g-PCA-PTX conjugate (Figure 2D) showed a completely different pattern in comparison with paclitaxel and MWNT-g-PCA as



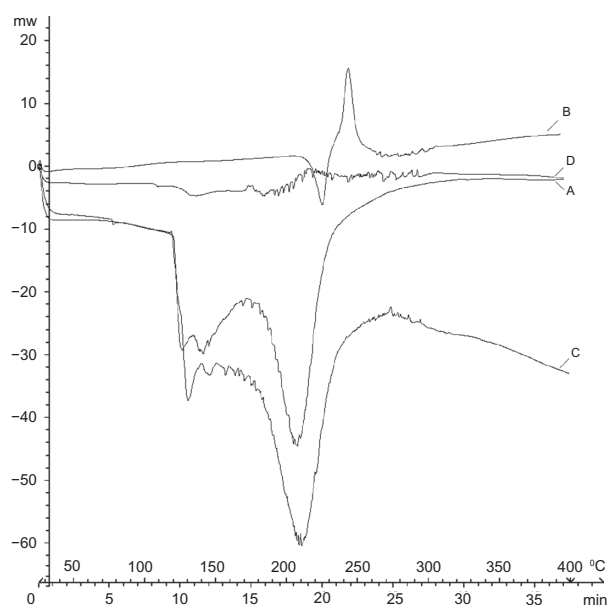


**Figure 2** Differential scanning calorimetry thermograms of **A)** MWNT-g-PCA, **B)** paclitaxel, **C)** physical mixture of MWNT-g-PCA and paclitaxel (1:1 w/w), and **D)** MWNT-g-PCA-PTX conjugates containing 40% w/w paclitaxel. **Abbreviations:** MWNT, multiwalled carbon nanotube; PCA, poly citric acid; PTX, paclitaxel.

precursors. The differential scanning calorimetry curve of the MWNT-g-PCA-PTX conjugate contained a large number of endothermic peaks starting at 180°C. The different pattern for the differential scanning calorimetry thermogram of MWNT-g-PCA-PRX referred to the nonhomogeneous structure and several objects that were conjugated together in a core shell-like hybrid nanomaterial. To emphasize that paclitaxel is not absorbed on MWNT-g-PCA physically but rather conjugated to it, a differential scanning calorimetry thermogram of a physical mixture of MWNT-g-PCA and paclitaxel (1:1 w/w) was compared with the MWNT-g-PCA-PTX conjugate. As can be seen in Figure 2C and Figure 2D, there is a big difference between the two thermograms. In the differential scanning calorimetry curve of the MWNT-g-PCA-PTX conjugate (Figure 2D), peaks of parent molecules (paclitaxel and MWNT-g-PCA) disappeared and a new profile was obtained, while in the physical mixture of MWNT-g-PCA and paclitaxel (Figure 2C) large endothermic peaks of MWNT-g-PCA covered the related peaks of paclitaxel. These results demonstrated that paclitaxel is conjugated to MWNT-g-PCA covalently.

### Particle size and polydispersity

Size and polydispersity of the conjugated nanotubes was evaluated using dynamic laser light scattering. The size of MWNT-g-PCA in water was about 125 nm and that of MWNT-g-PCA-PTX was about 207 nm (supplementary

data Figure S4), suggesting no significant aggregation of the MWNT-g-PCA after conjugation of the hydrophobic drug molecules. In order to confirm that dynamic light scattering produces the morphology and size of conjugated nanotubes, the nanotubes were further investigated using atomic force microscopy and transmission electron microscopy.

### Shape and surface morphology

Figure 3 shows atomic force microscopy images of oxidized MWNTs, MWNT-g-PCA, and MWNT-g-PCA-PTX dispersed on the surface of mica wafers. The atomic force microscopy image of oxidized MWNTs (Figure 3A) showed that the carbon nanotubes were in their extended conformation as linear or fiber shapes. They each had a length of several micrometers and a height of approximately 10 nm. Interestingly, atomic force microscopy images of MWNT-g-PCA (Figures 3B–D) did not show any linear or filamentous objects. It appears that the conjugated nanotubes were either in their closed or packed conformation with a disc-like morphology. The height and width of these nanostructures were 40–50 nm and 150 nm, respectively. Phase contrast imaging (Figure 3C and 3D) showed one phase for this hybrid material, confirming that the surface of the MWNT was covered by poly citric acid branches.

Topology images of the MWNT-g-PCA-PTX (Figure 3E) showed spherical nanostructures with a height and width of about 350 nm. However, phase contrast images of MWNT-g-PCA-PTX (Figure 3F and 3G) showed that spherical nanostructures observed in their topology images consisted of two or more self-assembled disc-like objects, with a size of approximately 100–130 nm.

Transmission electron microscopy images confirm the results of the atomic force microscopy observations. Figure 4 shows transmission electron microscopy images of MWNT-g-PCA-PTX. As shown, these particles are self-assembling toward spherical nanostructures, and no linear conformation for MWNTs could be seen.

### In vitro drug release

Due to the variability of the pH from 7.4 in extracellular parts of normal tissues, ie, 6.8 in tumor tissues and 5.0 in endosomes and lysosomes,<sup>30</sup> the release profiles of paclitaxel from the MWNT-g-PCA-PTX conjugates were evaluated at all the aforementioned pHs in the presence of 0.1% (w/w) Tween 80 for maintaining sink conditions. At sink conditions, the theoretical highest concentration of the drug in the medium is well below the 15% drug aqueous solubility. The aqueous solubility of paclitaxel is very low, and addition

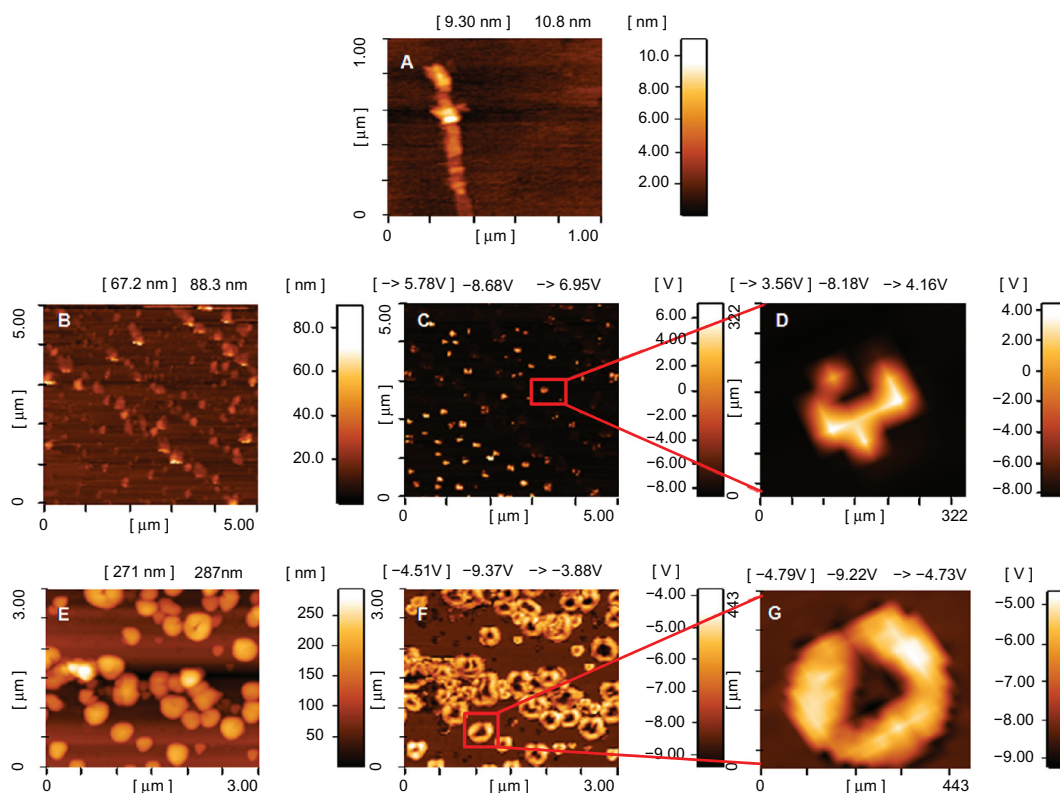


**Figure 3** Atomic force microscopy images of **A)** oxidized MWNTs, **B–D)** MWNT-g-PCA and **E–G)** MWNT-g-PCA-PTX conjugates on mica surface. **A, B, and E** are topographic and **C, D, F, and G** are phase contrast images.

**Abbreviations:** MWNT, multiwalled carbon nanotube; PCA, poly citric acid; PTX, paclitaxel.

of surfactants to the release medium increases its solubility. Therefore, the sink condition was maintained by the addition of Tween 80 and the frequent replacement of fresh buffer during the experiment.

As shown in Figure 5, hydrolysis of ester bonds to release paclitaxel in deionized water was significantly slower than in phosphate-buffered solutions. The release of paclitaxel from the MWNT-g-PCA-PTX conjugates at pH 6.8 and 5.0 was higher than at pH 7.4 (12.5% and 22.2% at pH 6.8 and 5.0, respectively, compared with 10.2% at pH 7.4), which was suitable for the release of the drug in tumor tissues and tumor cells.

## In vitro cytotoxicity

To verify whether the paclitaxel-conjugated nanotubes were pharmacologically active, in vitro cytotoxicity tests were conducted on SKOV3 ovary and A549 lung cancer cell lines. Figure 6 shows the cell viability of SKOV3 and A549 cells incubated with paclitaxel and MWNT-g-PCA-PTX for 24 hours and 48 hours. MWNT-g-PCA-PTX exhibited similar cytotoxicity as paclitaxel at shorter incubation times. As shown in Figure 6A at 40 nM concentration, the

cytotoxicity of MWNT-g-PCA-PTX at 24 hours was equal to the effect of paclitaxel at 48 hours. In addition, at a comparable incubation time, MWNT-g-PCA-PTX showed a higher cytotoxic effect than paclitaxel ( $P < 0.05$ ). For instance, at 24 hours, the cytotoxicity of MWNT-g-PCA-PTX containing 40 nM of paclitaxel was approximately 20% greater than the effect of 40 nM of free paclitaxel in A549 cells (Figure 6A). Therefore, the MWNT-g-PCA-PTX conjugates exhibited more cytotoxicity when compared with free paclitaxel at shorter incubation times. The same observations were made in the SKOV3 cell line (Figure 6B). These results could be related to the increased cell penetration of paclitaxel when conjugated to the MWNT-g-PCA. Extending the exposure time of paclitaxel and MWNT-g-PCA-PTX to 96 and 120 hours provided sufficient time for the penetration of free paclitaxel. Thus, after 96 hours, the MWNT-g-PCA-PTX exhibited similar toxicity patterns as free paclitaxel in both cell lines (Figure 7). It should be noted that, at all concentrations, the cytotoxicity of MWNT-g-PCA-PTX was slightly higher than for paclitaxel alone ( $n = 3$ ,  $P < 0.05$ ). For example, at 5 nM, the cytotoxicity of MWNT-g-PCA-PTX was 13.3% higher than free paclitaxel in SKOV3 cells

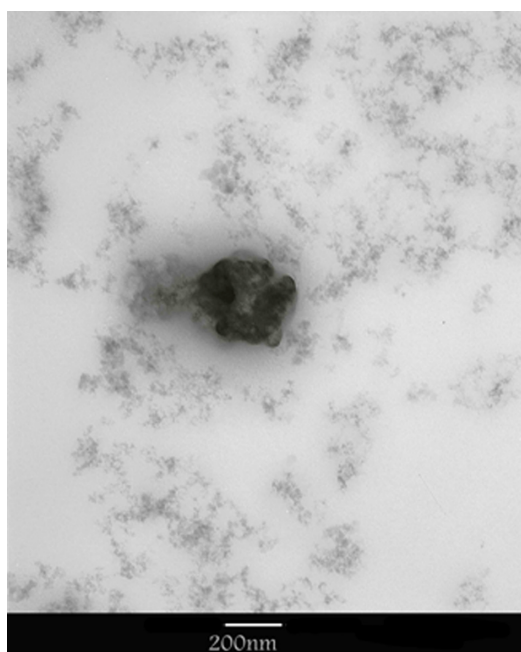


**Figure 4** Transmission electron microscopy images of MWNT-g-PCA-PTX conjugates.

**Abbreviations:** MWNT, multiwalled carbon nanotube; PCA, poly citric acid; PTX, paclitaxel.

at 96 hours of incubation time (Figure 7C). Moreover, the MWNT-g-PCA had no significant effect on cell viability at each incubation time, suggesting that the cytotoxicity was caused by the conjugated paclitaxel only. The calculated  $IC_{50}$ s for paclitaxel and the MWNT-g-PCA-PTX conjugate are summarized in Table 1.

## Discussion

Due to the three-dimensional structure of paclitaxel in which aromatic rings are not in a plane, there is not a strong noncovalent or  $\pi$ - $\pi$  interaction between paclitaxel and carbon nanotubes, as well as doxorubicin.<sup>11,20</sup> Although

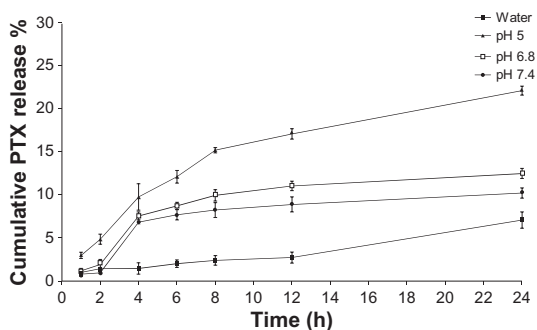


**Figure 5** Release profiles of paclitaxel from MWNT-g-PCA-PTX conjugates at preselected time intervals. Data are presented as means  $\pm$  standard deviations ( $n = 3$ ). **Abbreviations:** MWNT, multiwalled carbon nanotubes; PCA, poly citric acid; PTX, paclitaxel.

some research groups have reported physically loading of paclitaxel on CNTs-g-PEG in a saturated methanolic solution of paclitaxel using sonication,<sup>31</sup> in our study paclitaxel was covalently attached to the surface of MWNTs. Poly citric acid was chosen as a spacer to conjugate paclitaxel on the surface of MWNTs. Poly citric acid is a highly hydrophilic polymer that decreases the hydrophobicity of MWNTs. Poly citric acid is also a highly functional polymer with a large number of carboxylic functional groups that confer MWNTs with a high loading capacity. Moreover, poly citric acid is a highly biocompatible polymer.<sup>32,33</sup> Results of infrared,  $^1H$  NMR, and  $^{13}C$  NMR confirmed conjugation of paclitaxel to the carboxyl functional groups of the poly citric acid branches on the surface of MWNTs via a cleavable ester bond.

The size of a MWNT-g-PCA-PTX was about 207 nm, showing that MWNTs were not in their extended conformation, given that the length of MWNTs is known to be more than several hundred nanometers. Due to the hydrophobicity of MWNTs and hydrophilicity of poly citric acid in aqueous solutions, poly citric acid branches surrounding MWNTs causing conformational changes to curved nanotubes; thus, their size was much smaller than expected. In order to confirm the dynamic light scattering results, the morphology and size of the conjugated nanotubes were further investigated using atomic force microscopy and transmission electron microscopy. Atomic force microscopy images of MWNT-g-PCA and MWNT-g-PCA-PTX did not show a linear or extended structure for MWNTs. As mentioned previously, due to the high hydrophobicity of MWNTs and high hydrophilicity of poly citric acid, and in order to decrease interactions between MWNTs and water molecules, it appears that MWNT-g-PCA in aqueous solution adapts a conformation whereby carbon nanotubes have the lowest interaction with the solvent. When these forms of nanoparticles reacted with the hydrophobic drug, paclitaxel, molecular self-assembly was still retained. Solvent evaporation, occurring during sample preparation for atomic force microscopy and transmission electron microscopy imaging, caused the aggregation of conjugated nanotubes, which produced larger nanoparticles. Thus, grafting poly citric acid on the surface of MWNTs not only raised their water solubility and ability to be processed, but also changed their conformation toward new nanostructures for desired applications. As reported earlier in a similar study, the noncovalent interactions between polyglycerol and MWNTs changed the conformation of MWNTs from a linear toward a circular type.<sup>34</sup>

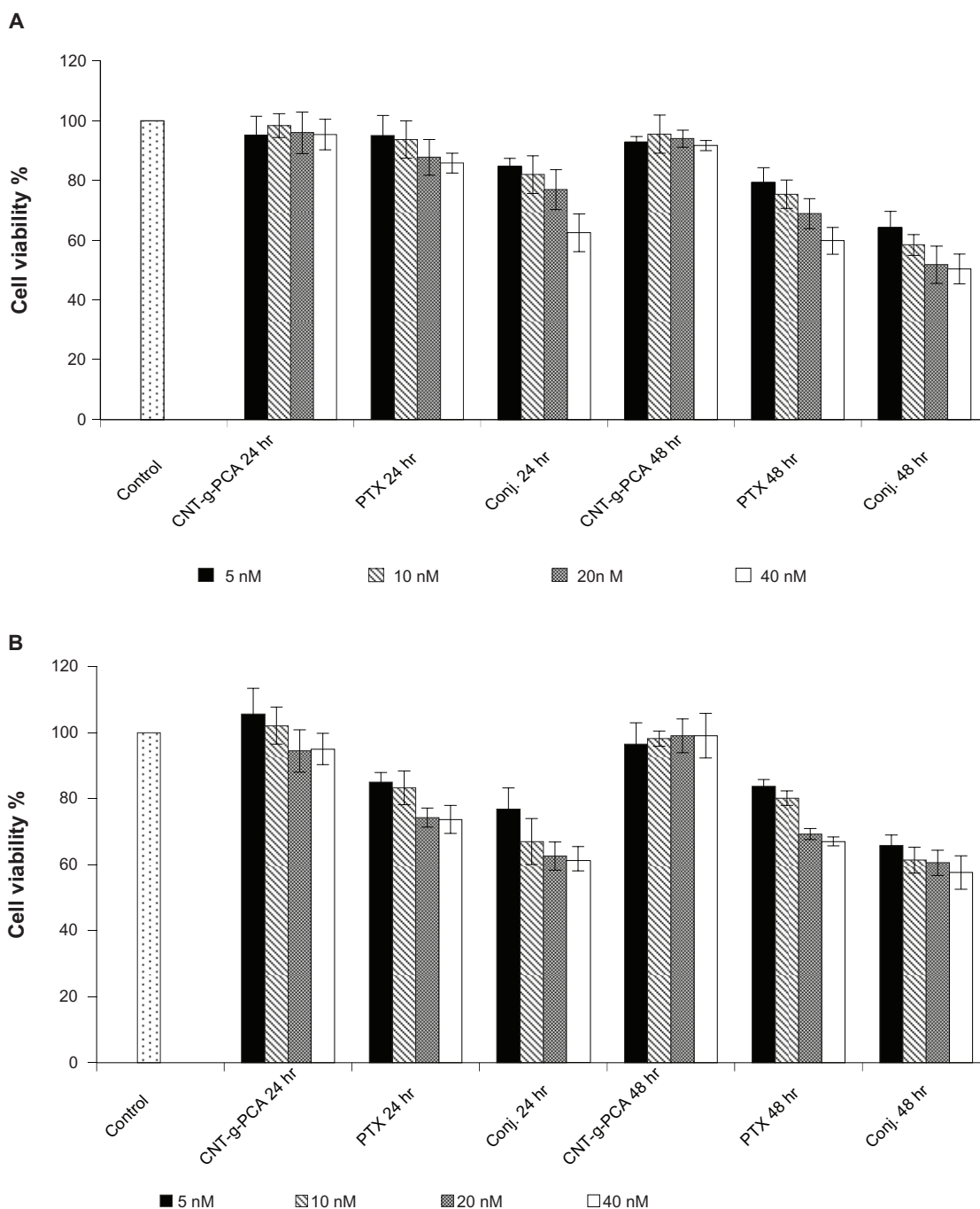


**Figure 6** Cytotoxicity of conjugated MWNT-g-PCA, MWNT-g-PCA-PTX, and paclitaxel against A549 (A) and SKOV3 (B) cells at 5, 10, 20, and 40 nM drug concentrations. Incubation time was 24 hours and 48 hours. Data are presented as means  $\pm$  standard deviations ( $n = 3$ ).

**Abbreviations:** MWNT, multiwalled carbon nanotube; PCA, poly citric acid; PTX, paclitaxel.

Drug content of paclitaxel in the MWNT-g-PCA-PTX conjugates was high enough to release an anticancer drug in the acidic environment of tumor cells and lysosomes. It seems that steric hindrance of hyperbranched poly citric acid decreased the rate of release in degradation. Similar results are reported in the literature when paclitaxel was conjugated to macromolecules or polymers

via ester bonds. Chemical degradation of ester bonds to release paclitaxel was performed at a slow rate in various pH levels.<sup>35–37</sup> In addition, hydrolysis of ester bonds to release paclitaxel from the conjugate form takes place via both chemical and enzymatic mechanisms. Thus, the esterase enzymes in the in vivo systems, especially in the lysosomes, will improve release of paclitaxel from the



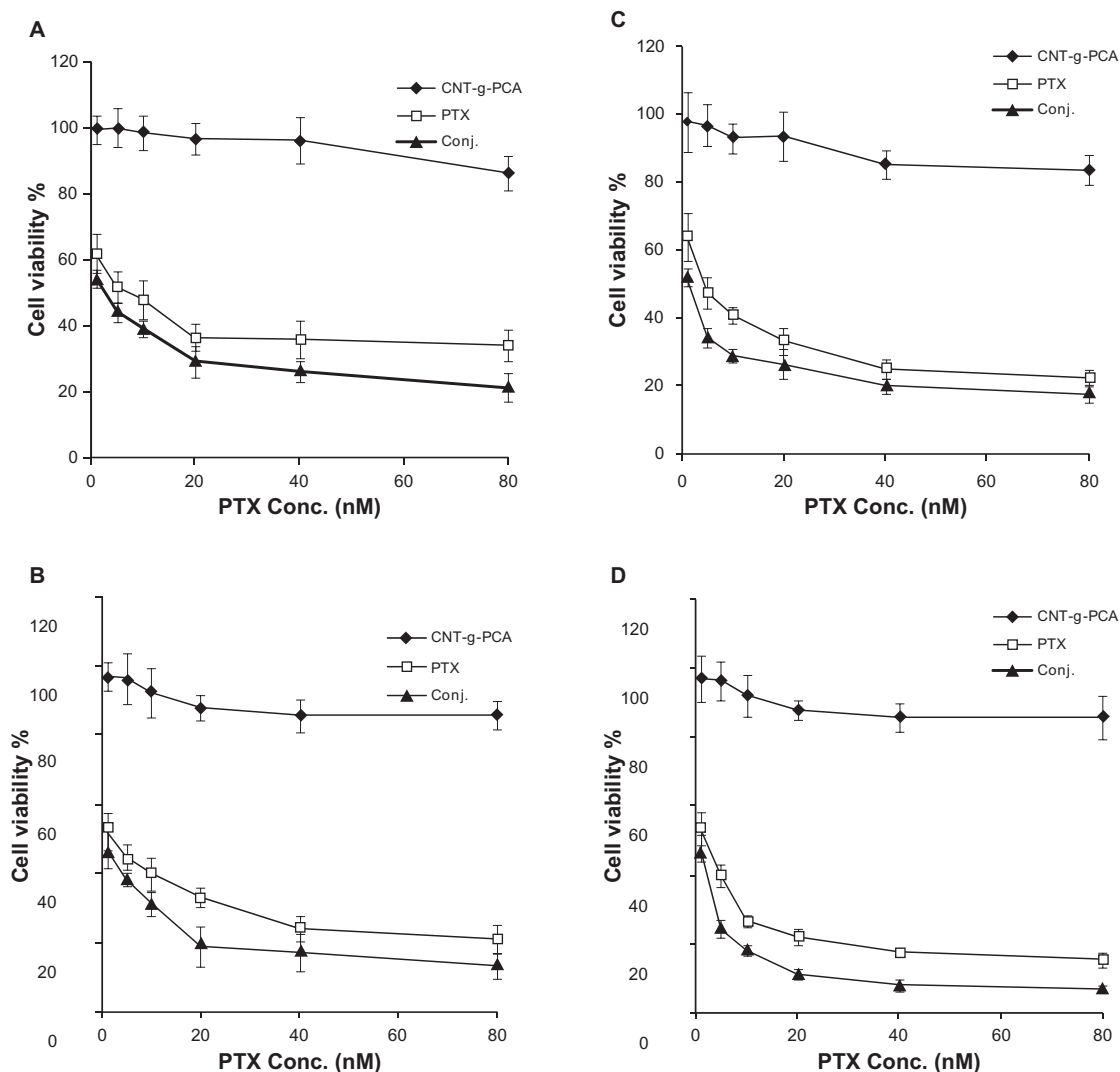


**Figure 7** Cytotoxicity of MWNT-g-PCA, MWNT-g-PCA-PTX, and paclitaxel against A549 (**A, B**) and SKOV3 (**C, D**) cells. Incubation time was 96 hours in **A** and **C**, and 120 hours in **B** and **D**. Data are presented as means  $\pm$  standard deviations ( $n = 3$ ).

**Abbreviations:** MWNT, multiwalled carbon nanotubes; PCA, poly citric acid; PTX, paclitaxel.

functionalized MWNTs through enzymatic hydrolysis in the tumor cells.

Cytotoxicity studies showed that MWNT-g-PCA-PTX conjugates exhibited a more cytotoxic effect in comparison with free drug, particularly during shorter time incubations.

Due to slow release of paclitaxel from the MWNT-g-PCA-PTX conjugate, at the proposed concentration, the amount of free drug in MWNT-g-PCA-PTX was much lower than that of free paclitaxel. Thus, the improved cytotoxic effect on the cancer cell lines may be due to higher cell penetration

**Table I**  $IC_{50}$ s (nM) of paclitaxel and conjugated MWNT-g-PCA-PTX against A549 and SKOV3 cell lines at different incubation times

Incubation time (hours)	A549		SKOV3	
	PTX	Conj	PTX	Conj
24	>2000*	>2000	>2000	>2000
48	>200	26.365 $\pm$ 2.685	>2000	>2000
96	6.686 $\pm$ 0.665	2.621 $\pm$ 0.165	4.211 $\pm$ 0.335	1.385 $\pm$ 0.074
120	2.063 $\pm$ 0.162	<1**	2.006 $\pm$ 0.096	<1

**Notes:** Data are presented as means  $\pm$  standard deviations ( $n = 3$ ). \* $IC_{50}$ s were obtained by extrapolation if the nonlinear regression was more than 2000 or 200 nM; \*\* $IC_{50}$ s in this incubation time was smaller than the lowest concentration used (1 nM).

**Abbreviations:** PTX, paclitaxel; Conj, conjugate; MWNT, multiwalled carbon nanotubes; PCA, poly citric acid.

of the conjugated nanotubes. This behavior could be related to amphiphilicity of the MWNT-g-PCA for improved cell wall interaction compared with absolute hydrophobic paclitaxel, the unique conformation of the conjugated nanotubes, or the carbon nanotube-based nanocarrier, which can penetrate into various cells.<sup>1,38</sup>

Nanoparticles can escape from the vasculature through the leaky endothelial tissue that surrounds the tumor and then accumulate in certain solid tumors by the so-called enhanced permeation and retention effect.<sup>39</sup> When paclitaxel is conjugated to MWNT-g-PCA nanohybrids, it can reach the tumor site via an enhanced permeability and retention effect. According to increased cell penetration, it can be considered that to reach a similar effect of drug, a much lower dose of MWNT-g-PCA-PTX than the commercial formulations of paclitaxel can be used. Decreasing the anticancer dose is highly favorable for lowering toxic side effects of drug therapy to the normal organs and tissues.

## Conclusion

In this study, MWNT-g-PCA was synthesized and used as a carrier for the anticancer drug, paclitaxel. During functionalization of MWNTs with poly citric acid, the conformation of the nanotubes changed from a linear toward a circular type. The release of paclitaxel from the MWNT-g-PCA-PTX conjugates at pH 6.8 and 5.0 was higher than at pH 7.4, which was suitable for the release of the drug in tumor tissues and tumor cells. Results of cytotoxicity assays demonstrated that MWNT-g-PCA-PTX exhibited a higher cytotoxic effect compared with unconjugated paclitaxel, which may be due to increased cell penetration. Based on these results, it can be concluded that the conjugation of paclitaxel to MWNT-g-PCA is an effective delivery system for cancer chemotherapy.

## Acknowledgment

The authors would like to thank Mr H Akbari and Mrs S Tavajohi for their laboratory work.

## Disclosure

The authors report no conflicts of interest in this work.

## References

- Pantarotto D, Singh R, McCarthy D, et al. Functionalized carbon nanotubes for plasmid DNA gene delivery. *Angewandte Chemie*. 2004; 43(39):5242–5246.
- Klumpp C, Kostarelos K, Prato M, Bianco A. Functionalized carbon nanotubes as emerging nanovectors for the delivery of therapeutics. *Biochim Biophys Acta*. 2006;1758(3):404–412.
- Merkoc A. Carbon nanotubes in analytical sciences. *Microchim Acta*. 2006;152:157–174.
- Ashok Kumar N, Ganapathy HS, Kim JS, Jeong YS, Jeong YT. Preparation of poly 2-hydroxyethyl methacrylate functionalized carbon nanotubes as novel biomaterial nanocomposites. *Eur Polym J*. 2008; 44(3):579–586.
- Liu Z, Tabakman S, Welscher K, Dai H. Carbon nanotubes in biology and medicine: In vitro and in vivo detection, imaging and drug delivery. *Nano Res*. 2009;2(2):85–120.
- Matsumura S, Ajima K, Yudasaka M, Iijima S, Shiba K. Dispersion of cisplatin-loaded carbon nanohorns with a conjugate comprised of an artificial peptide aptamer and polyethylene glycol. *Mol Pharm*. 2007; 4(5):723–729.
- Endo M, Strano M, Ajayan P. Potential applications of carbon nanotubes. In: *Topics in Applied Physics*. Berlin/Heidelberg: Springer-Verlag; 2008:13–62.
- Murakami T, Ajima K, Miyawaki J, Yudasaka M, Iijima S, Shiba K. Drug-loaded carbon nanohorns: Adsorption and release of dexamethasone in vitro. *Mol Pharm*. 2004;1(6):399–405.
- Son SJ, Bai X, Lee SB. Inorganic hollow nanoparticles and nanotubes in nanomedicine. Part 1. Drug/gene delivery applications. *Drug Discov Today*. 2007;12(15/16):650–656.
- Wang X, Ren J, Qu X. Targeted RNA interference of cyclin a2 mediated by functionalized single-walled carbon nanotubes induces proliferation arrest and apoptosis in chronic myelogenous leukemia K562 cells. *Chem Med Chem*. 2008;3(6):940–945.
- Liu Z, Sun X, Nakayama-Ratchford N, Dai H. Supramolecular chemistry on water-soluble carbon nanotubes for drug loading and delivery. *ACS Nano*. 2007;1(1):50–56.
- McDevitt MR, Chattopadhyay D, Kappel BJ, et al. Tumor targeting with antibody-functionalized, radiolabeled carbon nanotubes. *J Nucl Med*. 2007;48(7):1180–1189.
- Venkatesan N, Yoshimitsu J, Ito Y, Shibata N, Takada K. Liquid filled nanoparticles as a drug delivery tool for protein therapeutics. *Biomaterials*. 2005;26(34):7154–7163.
- Yang W, Thordarson P, Gooding JJ, Ringer SP, Braet F. Carbon nanotubes for biological and biomedical applications. *Nanotechnology*. 2007; 18:1–12.
- Guo Y, Shi D, Cho H, et al. In vivo imaging and drug storage by quantum-dot-conjugated carbon nanotubes. *Adv Funct Mater*. 2008; 18(17):2489–2497.
- Pastorin G, Wu W, Wieckowski S, et al. Double functionalisation of carbon nanotubes for multimodal drug delivery. *Chem Commun (Camb)*. 2006;(11):1182–1184.
- Ren Y, Pastorin G. Incorporation of hexamethylmelamine inside capped carbon nanotubes. *Adv Mater*. 2008;20(11):2031–2036.
- Teker K, Sirdeshmukh R, Sivakumar K, et al. Applications of carbon nanotubes for cancer research. *Nanobiotechnology*. 2005;1(2):171–182.
- Bhirde AA, Patel V, Gavard J, et al. Targeted killing of cancer cells in vivo and in vitro with EGF-directed carbon nanotube-based drug delivery. *ACS Nano*. 2009;3(2):307–316.
- Ali-Boucetta H, Al-Jamal KT, McCarthy D, Prato M, Bianco A, Kostarelos K. Multiwalled carbon nanotube-doxorubicin supramolecular complexes for cancer therapeutics. *Chem Commun (Camb)*. 2008; 8(4):459–461.
- Wu W, Wieckowski S, Pastorin G, et al. Targeted delivery of amphotericin B to cells by using functionalized carbon nanotubes. *Angewandte Chemie*. 2005;44(39):6358–6362.
- Foldvari M, Bagonluri M. Carbon nanotubes as functional excipients for nanomedicines: II. Drug delivery and biocompatibility issues. *Nanomedicine*. 2008;4(3):183–200.
- Lin Y, Taylor S, Huaping LI, et al. Advances toward bioapplications of carbon nanotubes. *J Mater Chem*. 2004;14:527–541.
- Maeda H, Wu J, Sawa T, Matsumura Y, Hori K. Tumor vascular permeability and the EPR effect in macromolecular therapeutics. *J Control Release*. 2000;65(1–2):271–284.
- Liu Z, Chen K, Davis C, et al. Drug delivery with carbon nanotubes for in vivo cancer treatment. *Cancer Res*. 2008;68(16):6652–6660.

26. Adeli M, Bahari A, Hekmatara H. Carbon nanotube-graft-poly(citric acid) nanocomposites. *NANO: Brief Rep Rev.* 2008;3(1):1–8.
27. Osorio AG, Silveira ICL, Bueno VL, Bergmann CP. H<sub>2</sub>SO<sub>4</sub>/HNO<sub>3</sub>/HCl-functionalization and its effect on dispersion of carbon nanotubes in aqueous media. *Appl Surf Sci.* 2008;255(5 Part 1):2485–2489.
28. Akhlaghi SP, Saremi S, Ostad SN, Dinarvand R, Atyabi F. Discriminated effects of thiolated chitosan-coated pMMA paclitaxel-loaded nanoparticles on different normal and cancer cell lines. *Nanomedicine.* 2010;6(5):689–697.
29. Chavanpatil MD, Patil Y, Panyam J. Susceptibility of nanoparticle-encapsulated paclitaxel to P-glycoprotein-mediated drug efflux. *Int J Pharm.* 2006;320(1–2):150–156.
30. Lee ES, Gao Z, Bae YH. Recent progress in tumor pH targeting nanotechnology. *J Control Release.* 2008;132(3):164–170.
31. Lay CL, Liu HQ, Tan HR, Liu Y. Delivery of paclitaxel by physically loading onto poly(ethylene glycol) (PEG)-graft-carbon nanotubes for potent cancer therapeutics. *Nanotechnology.* 2010;21(6):1–10.
32. Thomas LV, Arun U, Remya S, Nair PD. A biodegradable and biocompatible PVA-citric acid polyester with potential applications as matrix for vascular tissue engineering. *J Mater Sci Mater Med.* 2009; 20 Suppl 1:S259–S269.
33. Gyawali D, Nair P, Zhang Y, et al. Citric acid-derived in situ crosslinkable biodegradable polymers for cell delivery. *Biomaterials.* 2010;31(34):9092–9105.
34. Adeli M, Mirab N, Zabihi F. Nanocapsules based on carbon nanotubes-graft-polyglycerol hybrid materials. *Nanotechnology.* 2009; 20(48):1–10.
35. Cavallaro G, Licciardi M, Caliceti P, Salmaso S, Giammona G. Synthesis, physico-chemical and biological characterization of a paclitaxel macromolecular prodrug. *Eur J Pharm Biopharm.* 2004; 58(1):151–159.
36. Ceruti M, Crosasso P, Brusa P, Arpicco S, Dosio F, Cattel L. Preparation, characterization, cytotoxicity and pharmacokinetics of liposomes containing water-soluble prodrugs of paclitaxel. *J Control Release.* 2000;63(1–2):141–153.
37. Sugahara S, Kajiki M, Kuritama H, Kobayashi TR. Paclitaxel delivery systems: The use of amino acid linkers in the conjugation of paclitaxel with carboxymethyl dextran to create prodrugs. *Biol Pharm Bull.* 2002; 25(5):632–641.
38. Chin SF, Baughman RH, Dalton AB, et al. Amphiphilic helical peptide enhances the uptake of single-walled carbon nanotubes by living cells. *Exp Biol Med.* 2007;232(9):1236–1244.
39. Danhier F, Lecouturier N, Vroman B, et al. Paclitaxel-loaded PEGylated PLGA-based nanoparticles: In vitro and in vivo evaluation. *J Control Release.* 2009;133(1):11–17.

## Supplementary figures

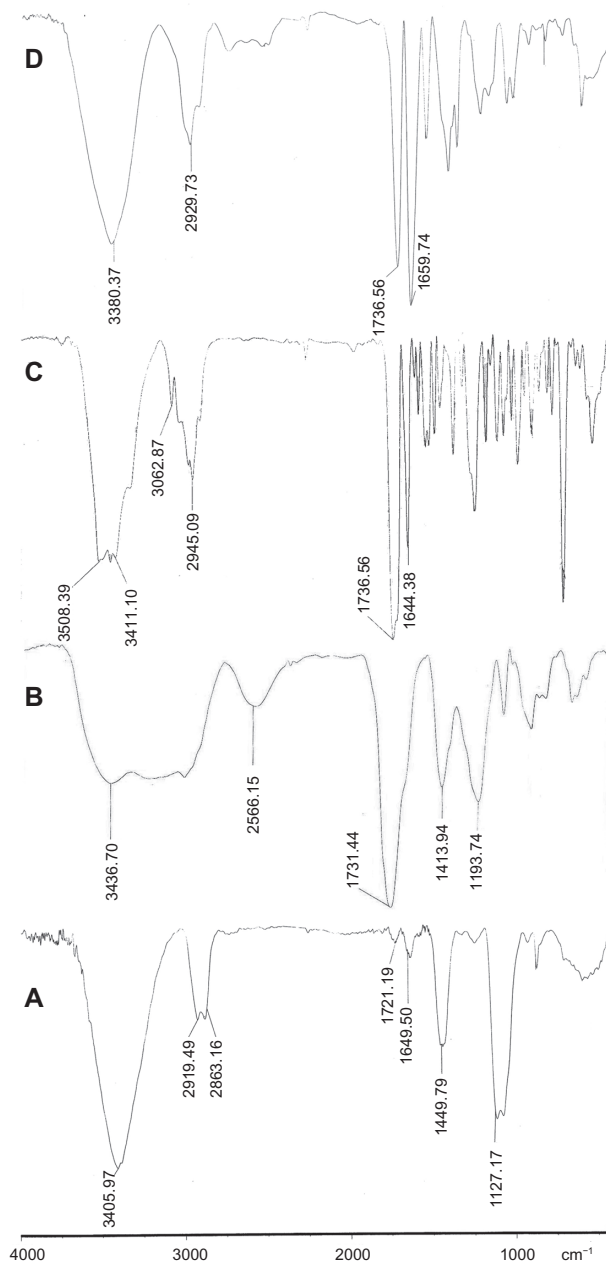


**Figure S1** Infrared spectra of the **A)** oxidized MWNTs, **B)** MWNT-g-PCA, **C)** PTX, and **D)** MWNT-g-PCA-PTX conjugates containing 40% w/w PTX. **Abbreviations:** MWNT, multiwalled carbon nanotube; PCA, poly citric acid; PTX, paclitaxel.



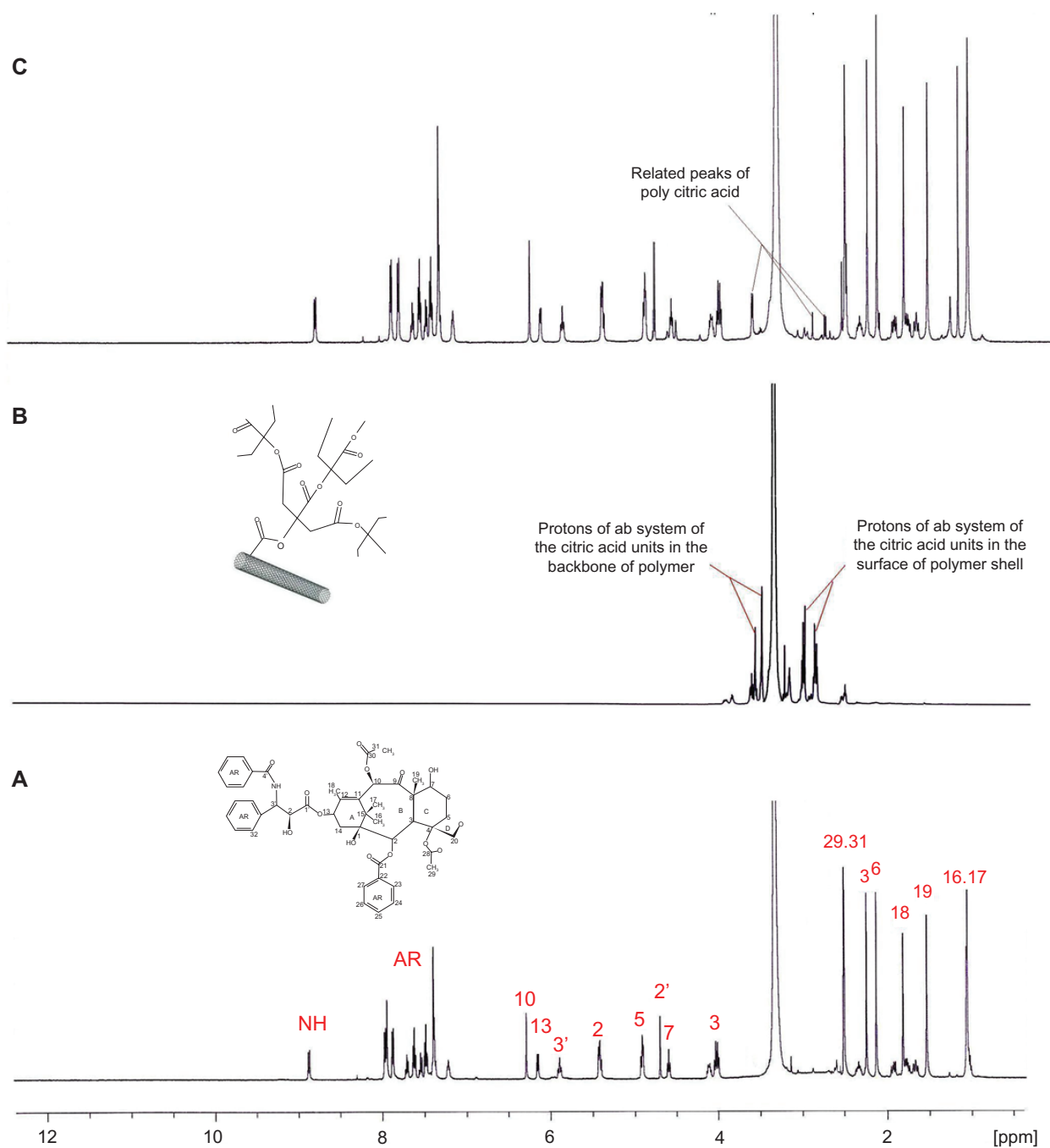


**Figure S2**  $^1\text{H}$  nuclear magnetic resonance spectra of **A)** paclitaxel, **B)** MWNT-g-PCA, and **C)** MWNT-g-PCA-PTX conjugates containing 40% w/w paclitaxel. **Abbreviations:** MWNT, multiwalled carbon nanotube; PCA, poly citric acid; PTX, paclitaxel.

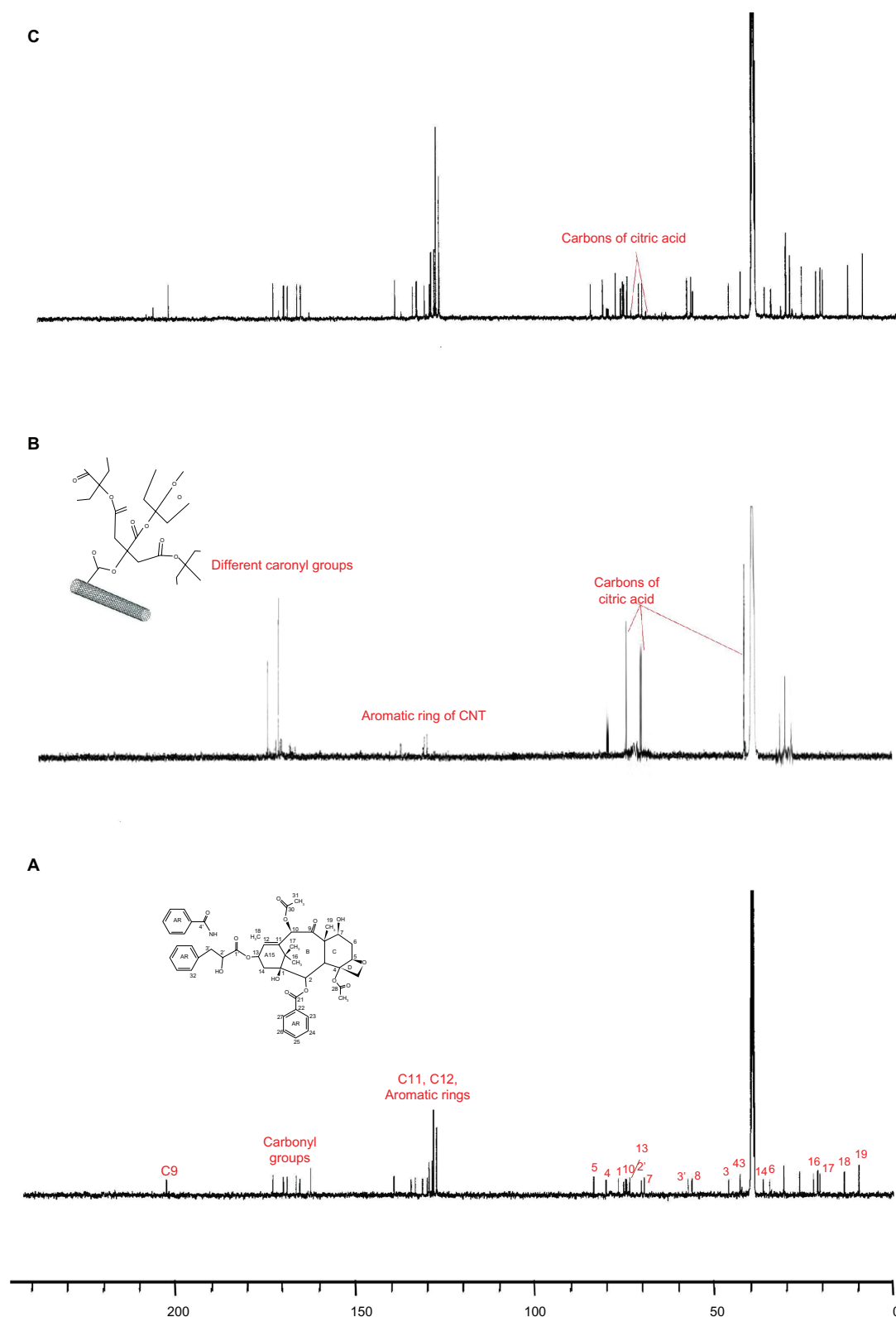


**Figure S3**  $^{13}\text{C}$  nuclear magnetic resonance spectra of **A)** PTX, **B)** MWNT-g-PCA, and **C)** MWNT-g-PCA-PTX conjugates containing 40% w/w paclitaxel. **Abbreviations:** MWNT, multiwalled carbon nanotube; PCA, poly citric acid; PTX, paclitaxel.

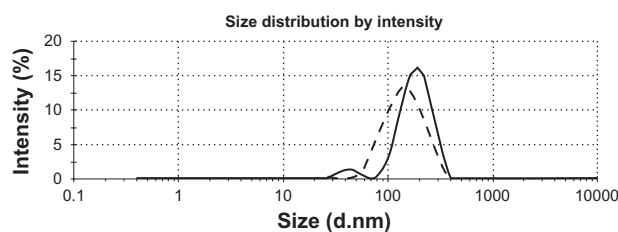


**Figure S4** Dynamic light scattering analysis of MWNT-g-PCA (dotted line) and MWNT-g-PCA-PTX conjugate (solid line).

**Abbreviations:** MWNT, multiwalled carbon nanotubes; PCA, poly citric acid; PTX, paclitaxel.

### International Journal of Nanomedicine

Dovepress

### Publish your work in this journal

The International Journal of Nanomedicine is an international, peer-reviewed journal focusing on the application of nanotechnology in diagnostics, therapeutics, and drug delivery systems throughout the biomedical field. This journal is indexed on PubMed Central, MedLine, CAS, SciSearch®, Current Contents®/Clinical Medicine,

Journal Citation Reports/Science Edition, EMBase, Scopus and the Elsevier Bibliographic databases. The manuscript management system is completely online and includes a very quick and fair peer-review system, which is all easy to use. Visit <http://www.dovepress.com/testimonials.php> to read real quotes from published authors.

Submit your manuscript here: <http://www.dovepress.com/international-journal-of-nanomedicine-journal>